

Conference on Quantum Electronics, Paris, 1962, edited by P. Grivet and N. Bloembergen (Columbia U. P., New York, 1964), p. 595.

¹⁴W. Low and R. S. Rubins, *Phys. Rev.* **131**, 2527 (1963).

¹⁵B. Bleaney, *Proc. Roy. Soc. (London)* **A277**, 289 (1964).

¹⁶M. Inoue, *Phys. Rev. Letters* **11**, 196 (1963).

¹⁷B. R. Judd and I. Lindgren, *Phys. Rev.* **122**, 1802 (1961).

¹⁸B. R. Judd, *Operator Techniques in Optical Spectroscopy* (McGraw-Hill, New York, 1963).

¹⁹R. E. Watson, P. Bagus, and A. J. Freeman, *Bull. Am. Phys. Soc.* **13**, 482 (1968).

²⁰B. Bleaney and K. W. H. Stevens, *Rept. Progr. Phys.* **16**, 108 (1953).

²¹H. E. Swanson, N. T. Gilfrich, and M. I. Cooke, *Natl. Bur. Std. (U.S.) Circ. No. 539*, **6** (1956); **7** (1957).

²²A. Zalkin and D. H. Templeton, *J. Chem. Phys.* **40**, 501 (1964).

²³J. Leciejewicz, *Z. Krist.* **121**, 158 (1965).

²⁴R. M. Curnutt and W. Viehmann (private communication).

²⁵M. L. Meil'man, M. I. Samoilovich, L. I. Potkin, and N. I. Sergeeva, *Fiz. Tverd. Tela* **8**, 233 (1966) [*Soviet Phys. Solid State* **8**, 1864 (1967)].

²⁶G. Feher, *Bell System Tech. J.* **36**, 449 (1957).

²⁷M. Abraham, R. A. Weeks, G. W. Clark, and C. B. Finch, *Phys. Rev.* **137**, A138 (1965).

²⁸J. Nemarich and W. Viehmann, *J. Phys. Chem. Solids* **29**, 57 (1968).

²⁹R. J. Elliot and K. W. H. Stevens, *Proc. Roy. Soc. (London)* **A218**, 553 (1953).

³⁰B. Bleaney, H. E. D. Scovil, and R. S. Trenam, *Proc. Roy. Soc. (London)* **A223**, 15 (1954).

³¹I. N. Kurkin, *Fiz. Tverd. Tela* **8**, 731 (1966) [*Soviet Phys. Solid State* **8**, 585 (1966)].

³²D. R. Mason, C. A. Morrison, C. Kikuchi, and R. T. Farrar, *Bull. Am. Phys. Soc.* **12**, 468 (1967).

³³L. Olschewski and E. W. Otten, *Z. Physik* **200**, 224 (1967).

³⁴J. M. Baker, W. B. J. Blake, and G. M. Copland, *Proc. Roy. Soc. (London)* **A309**, 119 (1969).

³⁵I. Lindgren, *Nucl. Phys.* **32**, 151 (1962).

³⁶A. J. Freeman and R. E. Watson, *Phys. Rev.* **127**, 2058 (1962).

Unusual Electron Paramagnetic Resonance Hyperfine Spectra of Yb³⁺ in Scheelites*

J. P. Sattler and J. Nemarich

Harry Diamond Laboratories, Washington D. C. 20438

(Received 19 January 1970)

The tetragonal *X* band electron paramagnetic resonance spectrum of Yb³⁺ shows an unusual hyperfine spectrum in the scheelite crystals SrWO₄, SrMoO₄, PbWO₄, and PbMoO₄. For these crystals, the principal $2I+1$ hyperfine absorption lines of the parallel spectrum do not go continuously into the $2I+1$ lines of the perpendicular spectrum as the angle of the magnetic field is varied from the crystal *c* axis. At some angles, more than the usual $2I+1$ transitions are observed. This unusual behavior is completely explained by the axial spin Hamiltonian $\mathcal{H} = g_{\parallel}\beta H_z S_z + g_{\perp}\beta(H_x S_x + H_y S_y) + AI_z S_z + B(I_x S_x + I_y S_y)$ and the relatively large ratio of B/A for Yb³⁺ in these crystals.

I. INTRODUCTION

The EPR spectrum of trivalent ytterbium in crystalline sites with tetragonal symmetry can be described by the spin Hamiltonian

$$\mathcal{H} = g_{\parallel}\beta H_z S_z + g_{\perp}\beta(H_x S_x + H_y S_y) + AI_z S_z + B(I_x S_x + I_y S_y), \quad (1)$$

where $S = \frac{1}{2}$, $I = 0$ for even-mass isotopes of ytterbium, and $I = \frac{1}{2}$ and $\frac{5}{2}$ for Yb¹⁷¹ and Yb¹⁷³, respectively. The parameters of this Hamiltonian have been measured for Yb³⁺ at *X* band and 4.2°K in a series of eight single crystals having the scheelite structure.¹ These measurements have included those for Yb³⁺ in tetragonal sites of cadmium molybdate, and of the tungstates and molybdates of calcium, strontium, and lead. In this paper, we

report on an unusual behavior of the hyperfine spectra observed in some of these crystals. For an ion with $S = \frac{1}{2}$, $2I+1$ absorption lines are usually observed. The isotopes Yb¹⁷¹ and Yb¹⁷³ exhibit this behavior in all scheelite crystals when the magnetic field is parallel or perpendicular to the crystal *c* axis. However, in some crystals, corresponding hyperfine absorption lines do not move continuously into one another as the magnetic field varies from the *c* axis to a perpendicular direction. Furthermore, four rather than two absorption lines are observed along some directions for Yb¹⁷¹. We have found that these spectra can be explained by the spin Hamiltonian of Eq. (1) with no additional terms, and are due to the large anisotropy of the hyperfine parameters observed for some of these crystals.

II. Yb^{3+} IN SCHEELITES

CaWO_4 , which may be considered a prototype for the structure of the scheelite family, is a tetragonal body-centered crystal. Its space group is classified as C_{4h}^6 ($I4_1/a$). Triply ionized ytterbium substitutes for the divalent cation, such as Ca^{2+} in CaWO_4 .² The site symmetry is tetragonal with point group S_4 .

The crystals used for this investigation were grown at this laboratory by the Czochralski technique. The crystal melt was doped with 0.05 at. % ytterbium and 0.2 at. % sodium, the latter added for charge compensation. Samples of several crystals were grown with enriched Yb^{171} or Yb^{173} to separate the resonance lines due to the various isotopes.

The tetragonal spectrum of Yb^{3+} in several scheelites has been reported.¹⁻⁵ The spectra in the tungstate and molybdate scheelites have been described by the spin Hamiltonian of Eq. (1) without inclusion of smaller terms such as those due to the nuclear Zeeman term, or for $I = \frac{5}{2}$, the nuclear quadrupole term.¹ The spin Hamiltonian parameters were found to vary in an approximately linear fashion with the crystal c -axis lattice constant. A summary of the values obtained for Yb^{171} in the tungstates and molybdates of calcium, strontium, and lead and for cadmium molybdate¹ is given in Table I. We note that g_{\parallel} and A decrease markedly with increasing value of c , whereas g_{\perp} and B decrease only slightly. The behavior of A and B for Yb^{173} is similar. Since the hyperfine interaction in Yb^{3+} is dipolar, the anisotropy in the A and B parameters is due to the anisotropy in the g factors.

III. EXPERIMENTAL PROCEDURE AND RESULTS

The measurements were made at 4.2 °K with a conventional X band superheterodyne spectrometer operating in the absorption mode. The sample cavity was a rectangular TE_{102} cavity provided with a mechanism which permitted rotation of the crystal in a vertical plane while immersed in liq-

uid helium. Using this device and a magnet mounted on a calibrated rotatable horizontal base, the angle θ between the crystalline c axis and the external magnetic field \vec{H} could be determined within a tenth of a degree.

As indicated above, for Yb^{3+} in all of the crystals listed in Table I, the expected nine-line spectrum was observed when the magnetic field was parallel or perpendicular to the crystal c axis. For CdMoO_4 , CaWO_4 , and CaMoO_4 , the parallel spectra went continuously into the perpendicular spectra as the angle of the magnetic field with the crystal c axis was varied. However, the spectra did not behave in this manner for the tungstates and molybdates of lead or strontium.

The spectra in these crystals are more easily described for the samples prepared with enriched Yb^{171} having $I = \frac{1}{2}$. The angular dependence of the spectrum of Yb^{171} in PbMoO_4 for the magnetic field oriented along or close to the crystal c axis is shown in Fig. 1. When the applied magnetic field is parallel to the c axis ($\theta = 0^\circ$), only the two strong lines labeled II and III appear. As θ increases, the two lines labeled I and IV appear. These new lines continue to grow in intensity as θ is increased, while the original resonances decrease in intensity. A weak resonance, corresponding to ytterbium of even-mass number can be seen between lines I and II at angles greater than 0.4° . When $\theta = 4.4^\circ$, the original resonances have become vestigial, and the resonances which were absent at $\theta = 0^\circ$ dominate the spectrum. Lines I and IV then move continuously with increasing θ into the two resonances seen when H is perpendicular to the c axis. Similar behavior was seen for Yb^{171} in PbWO_4 , SrMoO_4 , and SrWO_4 . This effect was not observed in CdMoO_4 , CaWO_4 , or CaMoO_4 . For these crystals, as has been described above, the two hyperfine lines seen in the parallel spectrum never died out with increasing θ but varied continuously into the two lines seen in the perpendicular spectrum. The spectra of Yb^{173} in the tungstates and molybdates of lead and strontium also showed extra lines. However, the angular variation spectrum for this isotope is not readily interpretable

TABLE I. Spin Hamiltonian parameters for Yb^{3+} in several crystals with scheelite structure (Ref. 1). The crystal c -axis lattice constants (Ref. 6) are also listed.

Crystal	c (Å)	g_{\parallel}	g_{\perp}	A^{171} (10^{-4} cm^{-1})	B^{171} (10^{-4} cm^{-1})
CdMoO_4	11.194	1.2393(1)	3.917(1)	310.0(3)	1027(1)
CaWO_4	11.376	1.0530(1)	3.916(1)	263.2(5)	1028(1)
CaMoO_4	11.43	0.9901(2)	3.912(1)	248(1)	1028(1)
SrWO_4	11.951	0.5966(3)	3.882(2)	141(3)	1023(3)
SrMoO_4	12.020	0.6131(2)	3.881(1)	149(1)	1023(1)
PbWO_4	12.046	0.6513(1)	3.886(1)	160(1)	1024(1)
PbMoO_4	12.106	0.6622(1)	3.883(1)	163(1)	1023(1)

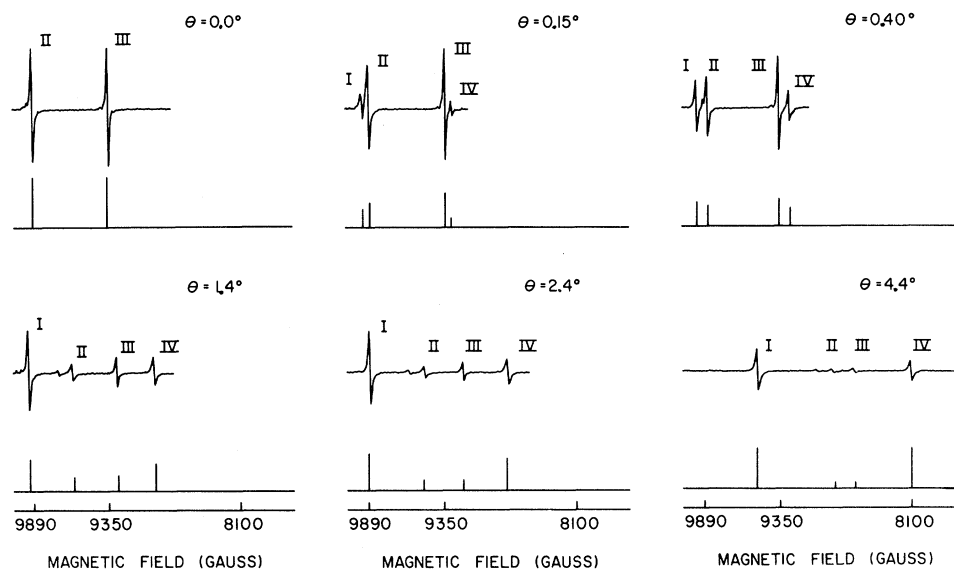


FIG. 1. Angular variation of the X band EPR spectrum of Yb^{171} in PbMoO_4 for the magnetic field parallel to ($\theta = 0.0^\circ$) and nearly parallel to the crystal c axis. The calculated absorption intensities are shown schematically below the experimental derivative absorptions.

due to overlapping lines, and it is not presented here.

IV. THEORY

We shall use CaWO_4 and PbMoO_4 as the prototypes of those crystals in which Yb^{171} exhibits, respectively, two or four hyperfine lines at X band. In either case, the spectrum may be fitted to the spin Hamiltonian given in Eq. (1), where $S = \frac{1}{2}$ and $I = \frac{1}{2}$. For the purpose of this discussion, we shall

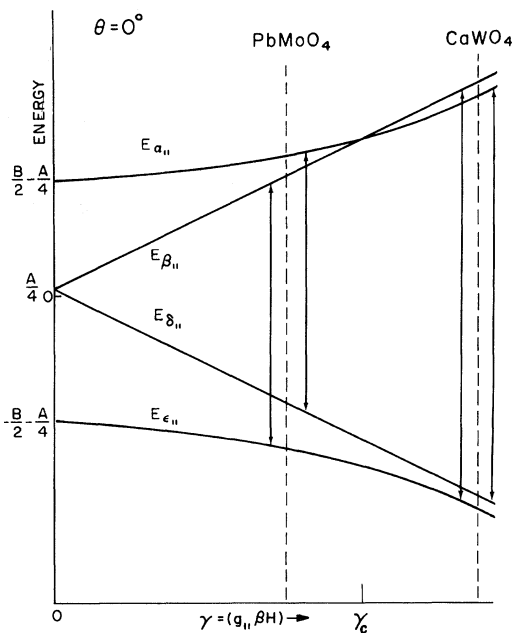


FIG. 2. Energy levels of Table II plotted versus $\gamma = g_{\parallel}\beta H$ assuming A and B positive. Allowed transitions and relative locations of resonances at X band for Yb^{171} in PbMoO_4 and CaWO_4 are shown.

assume that the external magnetic field moves in the crystal's x - z plane, where z or c designates the unique axis, and the linearly polarized microwave magnetic field is parallel to the y axis.

When the external magnetic field is parallel to the c axis, the energy levels and corresponding eigenfunctions are as given in Table II. As $\gamma = g_{\parallel}\beta H$ increases, the coefficient b decreases in magnitude, and the eigenfunctions more closely approximate the so-called "high-field" eigenfunctions. The hyperfine parameter B is responsible for the mixing of states in $|\psi_{\alpha\parallel}\rangle$ and $|\psi_{\epsilon\parallel}\rangle$.

Figure 2 shows a plot of the hyperfine energy levels versus γ for the case $\theta = 0^\circ$ assuming g_{\parallel} , A , and B positive and $B > A$. If B were less than or equal to A , $E_{\beta\parallel}$ would always be greater than $E_{\alpha\parallel}$. However, as shown in Table I, $B \approx 0.102 \text{ cm}^{-1}$ for all crystals considered here, whereas A ranges from 0.0310 to 0.0141 cm^{-1} . From the equations in Table II, one can easily show that $E_{\beta\parallel}$ will be greater than $E_{\alpha\parallel}$, only if $\gamma > \gamma_c$, where

$$\gamma_c = (B^2 - A^2)/2A. \quad (2)$$

Here γ_c is the value of γ at which levels $E_{\alpha\parallel}$ and $E_{\beta\parallel}$ cross. It can also be shown from the expressions for the energy levels and eigenfunctions given in Table II, that the hyperfine transitions for the parallel spectrum take place when

$$\gamma_{1,2} = [(2\sigma \pm A)^2 - B^2]/2(2\sigma \pm A). \quad (3)$$

The positive sign applies for γ_1 and the negative sign for γ_2 , and $\sigma = \nu/c$, where ν is the microwave frequency and c is the speed of light. If H_0 is the field for resonance for the $I=0$ isotope, then $\gamma_{1,2} = H_{1,2} \sigma/H_0$. The values of $\gamma_{1,2}$ occur below γ_c for PbMoO_4 , whereas they occur above γ_c for CaWO_4 .

TABLE II. Eigenvalues and eigenfunctions for the spin Hamiltonian of Eq. (1) with $S=\frac{1}{2}$, $I=\frac{1}{2}$ and the magnetic field parallel to crystal c axis ($\theta=0$). The eigenfunctions are expressed in the basis $|M_S, M_I\rangle$, and $\gamma=g_{\parallel}\beta H$.

$E_{\alpha\parallel} = \frac{1}{2}(\gamma^2 + B^2)^{1/2} - \frac{1}{4}A$
$ \psi_{\alpha\parallel}\rangle = a \frac{1}{2}, -\frac{1}{2}\rangle + b -\frac{1}{2}, \frac{1}{2}\rangle$
$E_{\beta\parallel} = \frac{1}{2}\gamma + \frac{1}{4}A$
$ \psi_{\beta\parallel}\rangle = \frac{1}{2}, \frac{1}{2}\rangle$
$E_{\delta\parallel} = -\frac{1}{2}\gamma + \frac{1}{4}A$
$ \psi_{\delta\parallel}\rangle = -\frac{1}{2}, -\frac{1}{2}\rangle$
$E_{\epsilon\parallel} = -\frac{1}{2}(\gamma^2 + B^2)^{1/2} - \frac{1}{4}A$
$ \psi_{\epsilon\parallel}\rangle = b \frac{1}{2}, -\frac{1}{2}\rangle + a -\frac{1}{2}, \frac{1}{2}\rangle$

As shown in Fig. 2, the allowed transitions occur between $\psi_{\alpha\parallel}$ and $\psi_{\delta\parallel}$ and between $\psi_{\beta\parallel}$ and $\psi_{\epsilon\parallel}$. For CaWO_4 , the transitions occur between the highest and lowest levels, and between the two intermediate levels, whereas for PbMoO_4 , transitions occur between alternate levels.

It is to be emphasized that we are not discussing merely high- versus low-field effects, since for $\nu \approx 9.2$ kHz, the hyperfine resonances for CaWO_4 occur in the neighborhood of 6 kG, whereas the resonances for PbMoO_4 occur at about 10 kG. Because of the difference in the magnitude of the g_{\parallel} factors, the so-called "high-field" case is better approximated in CaWO_4 at 6 kG than in PbMoO_4 at 10 kG.

When \vec{H} is no longer parallel to the c axis, the eigenfunctions are in general a linear combination of all four high-field states, and transitions between any two states cannot be ruled out.

When \vec{H} is perpendicular to the c axis, the energy levels and eigenfunctions are as given in Table III. The hyperfine energy levels are plotted versus $\gamma=g_{\perp}\beta H$ in Fig. 3. The allowed transitions

TABLE III. Eigenvalues and eigenfunctions for the spin Hamiltonian of Eq. (1) with $S=\frac{1}{2}$, $I=\frac{1}{2}$ and the magnetic field perpendicular to the crystal c axis ($\theta=90^\circ$). The eigenfunctions are expressed in the basis $|M_S, M_I\rangle$ and $\gamma=g_{\perp}\beta H$.

$E_{\alpha\perp} = \frac{1}{4}B + \frac{1}{2}[\gamma^2 + \frac{1}{4}(B-A)^2]^{1/2}$
$ \psi_{\alpha\perp}\rangle = a \frac{1}{2}, \frac{1}{2}\rangle + b \frac{1}{2}, -\frac{1}{2}\rangle + b -\frac{1}{2}, \frac{1}{2}\rangle + a -\frac{1}{2}, -\frac{1}{2}\rangle$
$E_{\beta\perp} = -\frac{1}{4}B + \frac{1}{2}[\gamma^2 + \frac{1}{4}(B+A)^2]^{1/2}$
$ \psi_{\beta\perp}\rangle = d \frac{1}{2}, \frac{1}{2}\rangle - c \frac{1}{2}, -\frac{1}{2}\rangle + c -\frac{1}{2}, \frac{1}{2}\rangle - d -\frac{1}{2}, -\frac{1}{2}\rangle$
$E_{\delta\perp} = \frac{1}{4}B - \frac{1}{2}[\gamma^2 + \frac{1}{4}(B-A)^2]^{1/2}$
$ \psi_{\delta\perp}\rangle = b \frac{1}{2}, \frac{1}{2}\rangle - a \frac{1}{2}, -\frac{1}{2}\rangle - a -\frac{1}{2}, \frac{1}{2}\rangle + b -\frac{1}{2}, -\frac{1}{2}\rangle$
$E_{\epsilon\perp} = -\frac{1}{4}B - \frac{1}{2}[\gamma^2 + \frac{1}{4}(B+A)^2]^{1/2}$
$ \psi_{\epsilon\perp}\rangle = -c \frac{1}{2}, \frac{1}{2}\rangle - d \frac{1}{2}, -\frac{1}{2}\rangle + d -\frac{1}{2}, \frac{1}{2}\rangle + c -\frac{1}{2}, -\frac{1}{2}\rangle$

are between $\psi_{\alpha\perp}$ and $\psi_{\delta\perp}$, and between $\psi_{\beta\perp}$ and $\psi_{\epsilon\perp}$. For all crystals, the transitions are between the highest and lowest level, and between the inner levels; transitions between alternate levels are strictly forbidden.

The appearance and disappearance of resonance lines for PbMoO_4 and the absence of this phenomenon for CaWO_4 may be understood by considering the variation of energy levels E with γ and θ . Surfaces in the E, γ, θ space can describe the situation, and Fig. 4 shows the projection of this surface on the γ - E plane. The energy levels for the parallel case are shown by solid lines, and the energy levels for the perpendicular case are shown by dashed lines. As θ varies from 0° to 90° , the energy levels vary through the appropriate shaded regions between the solid and dashed lines. The hyperfine energy levels as a function of γ for arbitrary θ are given by four curves, one lying in each shaded region. Here $\gamma=g\beta H$, where $g^2=g_{\parallel}^2\cos^2\theta + g_{\perp}^2\sin^2\theta$. For values of $\gamma < \gamma_c$, as θ varies from parallel to perpendicular, energy level $E_{\alpha\parallel}$ goes into $E_{\alpha\perp}$; however, for values of $\gamma > \gamma_c$, $E_{\alpha\parallel}$ goes into $E_{\beta\perp}$ with angular variation. This is a manifestation of the so-called "repulsion" of energy levels. Likewise, $E_{\beta\parallel}$ goes into $E_{\beta\perp}$ below the crossing point γ_c , but for $\gamma > \gamma_c$, $E_{\beta\parallel}$ moves into $E_{\alpha\perp}$ as θ is varied.

Figure 5 gives a schematic diagram of the variation of energy levels with angle θ , at constant γ , for PbMoO_4 and CaWO_4 . For PbMoO_4 at $\theta=0^\circ$,

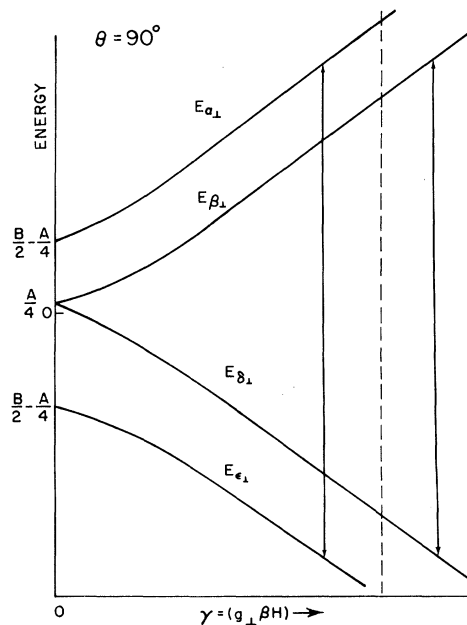


FIG. 3. Energy levels of Table III plotted versus $\gamma=g_{\perp}\beta H$ assuming A and B positive. Allowed transitions for Yb^{171} in scheelites are shown.

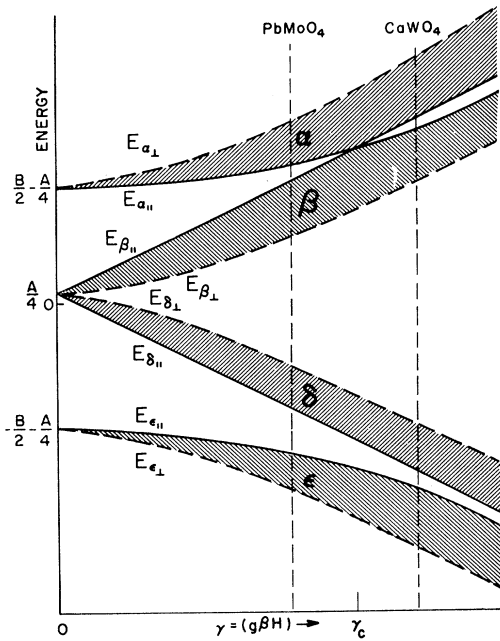


FIG. 4. Projection of the energy levels E versus θ on the E - γ plane, where θ is the angle between the crystal c axis and the magnetic field. The energy levels are for the spin Hamiltonian of Eq. (1) with $S = \frac{1}{2}$ and $I = \frac{1}{2}$ and A and B positive. Here $g = (g_{\parallel}^2 \cos^2 \theta + g_{\perp}^2 \sin^2 \theta)^{1/2}$. Curves for $\theta = 0^\circ$ and 90° are labeled, respectively, by $E_{\alpha\parallel}$ and $E_{\alpha\perp}$, etc.

the transition from level $E_{\delta\parallel}$ to level $E_{\alpha\parallel}$ corresponds to line II, whereas the transition from $E_{\epsilon\parallel}$ to $E_{\beta\parallel}$ corresponds to line III of Fig. 1. For the perpendicular case, the allowed absorption transitions are from $E_{\epsilon\perp}$ to $E_{\alpha\perp}$ and from $E_{\delta\perp}$ to $E_{\beta\perp}$, corresponding to lines IV and I, respectively, of Fig. 1. Since the variation of energy levels with angle is continuous, and the energy levels do not cross over each other as θ is varied from 0° to 90° , the resonances II and III seen for the parallel field must die out, and resonances I and IV, which become the perpendicular resonances, must grow. For CaWO_4 , the same selection rules hold. However, the ordering of levels $E_{\alpha\parallel}$ and $E_{\beta\parallel}$ is reversed from the PbMoO_4 case. Consequently, the resonance between $E_{\delta\parallel}$ and $E_{\alpha\parallel}$ can move continuously into the resonance between levels $E_{\delta\perp}$ and $E_{\beta\perp}$; likewise, the transition between $E_{\epsilon\parallel}$ and $E_{\beta\parallel}$ becomes the transition between $E_{\epsilon\perp}$ and $E_{\alpha\perp}$ as θ is varied. No transition need die out, and transitions always exist between the two inner energy levels, and between the two outer energy levels.

The identification of the lines of the spectra of Yb^{171} in PbMoO_4 , PbWO_4 , SrMoO_4 , and SrWO_4 was checked by diagonalizing the spin Hamiltonian (1) using the parameters of Table II at the fields and

angles of each observed line. It was confirmed in each instance that the observed transition was permitted by energy and angular momentum selection rules. For each observed transition, the energy difference was found to equal the microwave energy within experimental error. The intensity of the transitions was also calculated and found to agree with the observed intensities. The calculated results obtained for Yb^{171} in PbMoO_4 are shown schematically in Fig. 1 beneath the corresponding observed spectrum. For CaWO_4 , it is found that at any angle only two lines will have sufficient intensity to be seen in the X band spectrum, in accordance with the experiment.

V. CONCLUSION

An unusual behavior has been observed of the intensities of the X band spectra of Yb^{3+} in the single crystal scheelites SrWO_4 , SrMoO_4 , PbWO_4 , and PbMoO_4 . The spectra of crystals enriched with Yb^{171} having $I = \frac{1}{2}$ have been analyzed to determine the origin of the anomalous behavior. In contrast to a recent study where the appearance of "forbidden" lines was explained by adding to the axial spin Hamiltonian terms due to the interaction of the nuclear spin with the external field,⁷ no modification of the simple spin Hamiltonian given by Eq. (1) is needed here. Diagonalization of this Hamiltonian with the parameters given in Table I completely explains the observed angular variation of the spectra.

The unusual behavior of the spectra can be traced to the large ratio B/A of the hyperfine parameters. Since the hyperfine interaction for

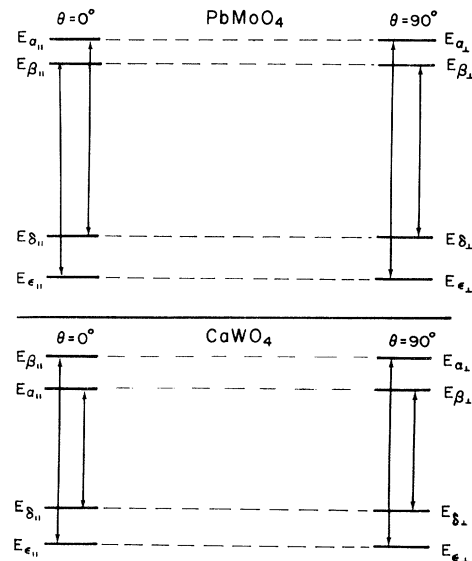


FIG. 5. Schematic diagram of the variation of energy levels with θ , at constant γ , for Yb^{171} in PbMoO_4 and CaWO_4 , respectively.

ytterbium is dipolar in nature, this large ratio of B/A is due to the large ratio of g_{\perp}/g_{\parallel} for these crystals. We note that the S band spectra of all these crystals, including CaWO_4 , would exhibit the unusual behavior similar to that described above. However, the K band spectra would exhibit the normal behavior observed for Yb^{3+} in CaWO_4 since γ would then be greater than γ_c .

ACKNOWLEDGMENTS

We would like to thank R. M. Curnutt, R. T.

Farrar, and W. Viehmann for preparation of the crystals used in this investigation, and Dr. N. Karayianis for helpful discussions and for use of his computer subroutines. One of us (J. P. S.) would like to thank Dr. L. Leopold for many valuable discussions. The crystals were x-ray oriented by A. J. Edwards, and D. L. Chambers provided technical assistance in construction of the spectrometer.

*Paper based on material submitted by J. P. Sattler in partial fulfillment of the requirements for the Ph.D. degree in physics, Georgetown University, Washington, D. C.

¹J. P. Sattler and J. Nemanich, preceding paper, Phys. Rev. B 1, 4249 (1970).

²U. Ranon and V. Volterra, Phys. Rev. 134, A1483 (1964).

³J. Kirton and R. C. Newman, Phys. Letters 10, 277 (1964).

⁴I. N. Kurkin and L. Ya. Shekun, Opt. i Spektroskopiya 18, 738 (1966) [Opt. Spectry (USSR) 18, 417 (1965)].

⁵A. A. Antipin, I. N. Kurkin, L. S. Potkin, and L. Ya. Shekun, Fiz. Tverd. Tela 8, 2808 (1966) [Soviet Phys. Solid State 8, 2247 (1967)].

⁶H. E. Swanson, N. T. Gilfrick, M. I. Cooke, Natl. Bur. Std. (U.S.) Circ. No. 539, 6 (1956); 7, (1957).

⁷S. H. Choh and G. Seidel, Phys. Rev. 164, 412 (1967).

Adiabatic Quantum Theory of Spin-Lattice Relaxation

Joseph Levy

Centre de Mécanique Ondulatoire Appliquée, 23, Rue du Maroc, Paris 19ème, France

(Received 14 October 1968; revised manuscript received 3 April 1969)

A theory of spin-lattice relaxation is presented in which the modulated crystalline potential does not act directly, but entails modulation of orientation and polarization of the orbitals. These factors are responsible for a modulation of the effective magnetic field acting on the electron spin, which supplies the spin transitions. Three consequences result from this formulation: (a) The spin Zeeman term does not play its traditional role in the relaxation process, the reason for this being that the effective dynamic magnetic field in Kramers salts is related to $\lambda \vec{L} \cdot \vec{S}$ and $\beta \vec{L} \cdot \vec{H}$, and not to $2\beta \vec{S} \cdot \vec{H}$. In other words, the relaxation results from the modulation of the anisotropic g factor. (b) The rotational modes of the crystalline complex may play an important role, even though the amplitude of vibration is weaker than that of the vibration modes. We will see indeed that the rotating motion of the orbitals can be essential in the relaxation process; this motion is generated by all the vibration modes (which also entail polarizations), but in particular by the purely rotational modes of the complex. (c) Another effect will result from the modulation of the orbital energy; this effect will be studied in an addendum [Phys. Rev. (to be published)].

I. INTRODUCTION

Since the work of Heitler and Teller¹ and Fierz² it has generally been admitted that spin-lattice relaxation in crystalline media is, principally, a process by which the modulated potential (gener-

ated by the thermal motion of the lattice atoms) supplies transitions between the spin eigenstates of the static Hamiltonian,³ the energy difference being transferred to the lattice oscillators. This way of considering the problem implies the hypoth-